Dalton Transactions

Accepted Manuscript

ROYAL SOCIETY OF CHEMISTRY

www.rsc.org/dalton

Graphical Abstract

Influence of central metal ion in controlling the self-assembly and magnetic properties of 2D coordination polymers derived from $[(NiL)_2M]^{2+}$ nodes (M = Ni, Zn and Cd) (H_2L = salen type di-Schiff base) and dicyanamide spacers

Lakshmi Kanta Das, Carlos J. Gómez-García and Ashutosh Ghosh*

Three new 2D coordination polymers of different network with significant variation in the magnetic properties have been synthesized by changing the central metal in the trinuclear nodes.

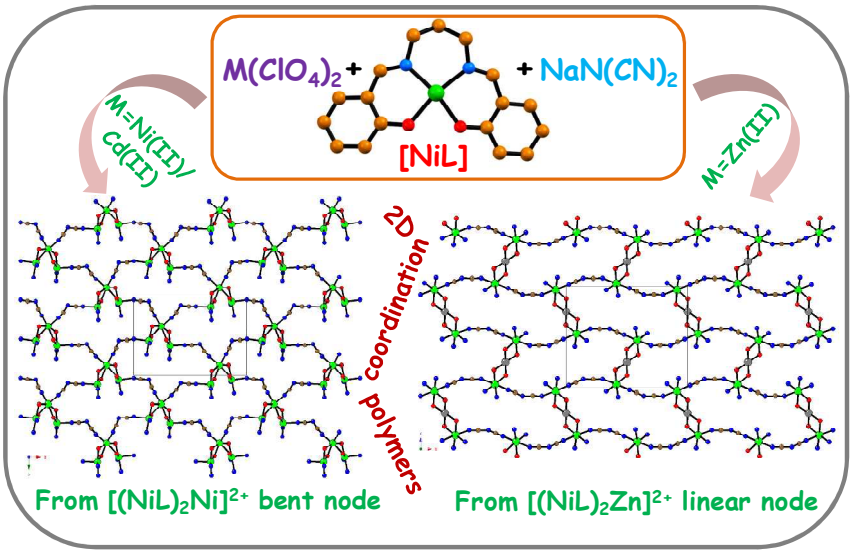

Influence of central metal ion in controlling the self-assembly and magnetic properties of 2D coordination polymers derived from $[(NiL)_2M]^{2+}$ nodes (M = Ni, Zn and Cd) (H_2L = salen type di-Schiff base) and dicyanamide spacers

Lakshmi Kanta Das[a], Carlos J. Gómez-García[b] and Ashutosh Ghosh[a]*

Received (in XXX, XXX) XthXXXXXXXXX 20XX, Accepted Xth XXXXXXXXX 20XX
DOI: 10.1039/b000000x

Three new 2D coordination polymers (CPs) $^2{}_\infty[(NiL)_2Ni(\mu_{1,5}\text{-}N(CN)_2)_2]_n$ (**1**), $^2{}_\infty[(NiL)_2Cd(\mu_{1,5}\text{-}N(CN)_2)_2]_n$ (**2**) and $^2{}_\infty[(NiL)_2Zn(\mu_{1,5}\text{-}N(CN)_2)_2]_n$ (**3**) have been synthesized by reacting a [NiL] "metalloligand" (where H_2L = N,N'-bis(salicylidene)-1,3-propanediamine) with three different metal(II) (Ni, Cd and Zn) perchlorate and sodium dicyanamide, with identical molar ratio of the reactants. All three products have been characterized by IR and UV-Vis spectrscopies, elemental analyses, powder and single crystal X-ray diffraction and variable temperature magnetic measurements. The isomorphous compounds **1** and **2** consist of similar $[(NiL)_2M(\mu_{1,5}\text{-}N(CN)_2)]$ (M = Ni for **1** and Cd for **2**) angular trinuclear units in which two terminal "metalloligands" [NiL] coordinate to the central nickel(II) (in **1**) or cadmium(II) (in **2**) ion through phenoxido oxygen atoms. The $\mu_{1,5}$-bridging dicyanamido spacers connect the central Ni(II) or Cd(II) of one node to terminal Ni(II) of two different nodes giving rise to 2D CPs. Compound **3** also contains trinuclear units with the same formula as those of **1** and **2**: $[(NiL)_2M(\mu_{1,5}\text{-}N(CN)_2)]$ (M = Zn in **3**). The main differences are that these units are linear in **3** and the dicyanamide spacers link only the nickel atoms of neighbouring nodes. As in **1** and **2**, these trinuclear units are connected with four other units *via* four $\mu_{1,5}$-bridging dicyanamido ligands giving rise to 2D CP with a similar topology: an uninodal 4-connected underlying net with the **sql** (Shubnikov tetragonal plane net) topology and $(4^4.6^2)$ point symbol. The magnetic properties show the presence of moderate intra-trinuclear antiferromagnetic interactions in **1** (J = -12.9 cm^{-1}) and weak antiferromagnetic interactions between the terminals Ni(II) ions in **2** (J = -2.4 cm^{-1}). In **3** the Ni(II) ions are well isolated by the central Zn(II) ion and accordingly, only a very weak antiferromagnetic interactions through the single $\mu_{1,5}$-bridging dicyanamido ligands is observed (J = -0.44 cm^{-1}, D = -3.9 cm^{-1}).

Introduction

In the last decade, the design and construction of coordination polymers (CPs) are an emerging area of research due to their structural diversity and several potential applications in areas such as catalysis, conductivity, porosity, chirality, luminescence, magnetism, spin-transition and non-linear optics.[1] The CPs are an intriguing class of hybrid crystalline materials that are constructed by the spontaneous self-assembly of metal ions or clusters (node or connector) and organic ligands (linker or spacer) driven by metal-ligand coordination interaction that extend infinitely into one, two or three dimensions.[2] In the year 1990, Robson established and illustrated "the node-and-spacer approach"[3] which has been remarkably successful in producing various CPs with predictable network architectures and desired topologies. This can be easily achieved by choosing the metal ions according to their appropriate coordination number and geometry, charge and HSAB behaviour (concept of Hard and Soft Acids and Bases), as well as bridging spacers with suitable denticity, shape, size and flexibility.[4] Recently, we and others have shown that oligonuclear nodes are excellent building blocks in designing novel CPs due to their higher geometrical flexibility because of the presence of two or more metal ions.[5-8] In this regard, hetero-trinuclear (3d-3d′-3d,3d-3d-4f, 3d-3d′-4f, etc.) cationic or neutral compounds of cyclic as well as acyclic Schiff base ligands[5,6,9] deserve special mention as they can be used to construct polymers of various dimensionalities and topologies. Moreover, several important properties like magnetic, optical, redox or catalytic which depend upon metal–metal intra- and inter-node interactions[10] in the resulting CPs, can be modified by the introduction of the hetero-metal ions into the trinuclear nodes.[6,7]

Recently, we synthesized some hetero-metallic trinuclear compounds of general formula $\{[(ML)_2M'(N(CN)_2)_a]X_b\}$ (where M = Cu(II) or Ni(II), M′ = Co(II), Zn(II) or Cd(II), L= salen type di-Schiff base ligand, X = ClO_4^-, a = 1 or 2 and b = 1 or 0) and used them as nodes to construct CPs.[5,6] These trinuclear compounds are conformationally and coordinatively flexible. Depending upon the coordination geometry of the central metal ions and coordination mode of the anionic coligands, the trinuclear compounds can vary from linear to bent shapes leading to the different spatial orientation of the "metalloligand" in the trinuclear species. As a consequence, when such species are used as nodes the resulted CPs can be of various dimensions and topologies. For examples, using $\{[ML]_2M'\}^{2+}$, (M = Cu(II) or Ni(II), L= salen type di-Schiff base ligand and M′ = Co(II), Zn(II) or Cd(II)) as nodes and dicyanamide as spacers we succeeded to get species ranging from hexanuclear cluster to 1D to 2D to 3D polymers; some of which present very rare examples

of genuine supramolecular isomers.[5] We observed that besides the nature of central hetero-metal atoms, the dimension and topology of the coordination network depend also upon the coordination numbers of the terminal "metalloligands" and the different bridging modes and spatial orientation of the dicyanamide spacer.

Here in, we report the synthesis and structural features of three new 2D CPs $^{2}_{\infty}[(NiL)_2Ni(\mu_{1,5}\text{-}N(CN)_2)_2]_n$ (**1**), $^{2}_{\infty}[(NiL)_2Cd(\mu_{1,5}\text{-}N(CN)_2)_2]_n$ (**2**) and $^{2}_{\infty}[(NiL)_2Zn(\mu_{1,5}\text{-}N(CN)_2)_2]_n$ (**3**) (where H_2L = N,N′-bis(salicylidene)-1,3-propanediamine) assembled from the [NiL] "metalloligand", the dicyanamide spacer and metal salts of Ni(II), Cd(II) and Zn(II). Interestingly, the trinuclear nodes $[(NiL)_2M]^{2+}$ [M = Ni(II) for **1** and Cd(II) for **2**) of **1** and **2** adopt bent molecular shape whereas the trinuclear node, $[(NiL)_2Zn]^{2+}$ in **3** is linear (Scheme 1), in which two metalloligands are nearly perpendicular to each other making its shape unique. The variable-temperature magnetic susceptibility measurement of all three polymers is presented in detailed.

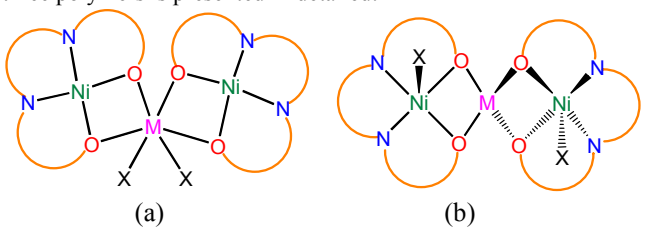

Scheme 1: Bent and Linear trinuclear nodes are resulted depending upon the coordination geometry of the central hetero-metal ions (M). (a) Octahedral environment of M (M = Ni(II) and Cd(II)) results bent node in which two "metalloligands" are almost parallel to each other (b) Tetrahedral environment of M (M = Zn(II)) results linear node where two "metalloligands" are nearly perpendicular to each other. Here, H_2L is N,N′-bis(salicylidene)-1,3-propanediamine and X is dicyanamide.

Experimental Section

Starting materials

All chemicals including salicylaldehyde and 1,3-propanediamine were purchased from Lancaster and were of reagent grade. They were used without further purification.

Caution! Perchlorate salts are potentially explosive. Only a small amount of material should be prepared and handled with care.

Synthesis of the Schiff base ligand N,N'-bis(salicylidene)-1,3-propanediamine (H_2L) and the "metalloligand" [NiL]

The Schiff base ligand was synthesized by standard methods: 5 mmol of 1,3-propanediamine (0.42 mL) were mixed with 10 mmol of salicylaldehyde (1.04 mL) in methanol (20 mL). The resulting solution was refluxed for *ca.* 2 h, and allowed to cool. The yellow methanolic solution was used directly for compound formation. An aqueous solution (20 mL) of $Ni(ClO_4)_2{\cdot}6H_2O$ (1.820 g, 5 mmol) and 10 mL ammonia solution (20%) were added to a methanolic solution of H_2L (10 mL, 5 mmol) to prepare the "metalloligand", [NiL] as reported earlier.[11]

Synthesis of $^{2}_{\infty}[(NiL)_2Ni(\mu_{1,5}\text{-}N(CN)_2)_2]_n$ (1)

The precursor "metalloligand" [NiL] (0.642 g, 2 mmol) was dissolved in methanol (20 mL) and then a water solution (1 mL) of $Ni(ClO_4)_2{\cdot}6H_2O$ (0.364 g, 1 mmol) followed by an aqueous solution (1 mL) of sodium dicyanamide (0.180 g, 2 mmol) were added to this solution. The mixture was stirred for 1 h at room temperature producing a suspension containing a green solid. This was filtered off, washed with methanol-water mixture and dried to give **1**. The filtrate was allowed to stand overnight at open atmosphere resulting in the formation of green prismatic shaped X-ray quality single crystals of **1**. These crystals were washed with methanol-water mixture and dried in a desiccator containing anhydrous $CaCl_2$ to give the second crop of **1**, and then characterized by elemental analysis, spectroscopic methods and X-ray diffraction.

Compound **1**: Yield: 0.773g, 89% (including the green precipitate and the crystalline compound). Anal. calc. for $C_{38}H_{32}Ni_3N_{10}O_4$: C 52.53, H 3.71, N 16.12 found: C 52.69, H 3.54, N 16.40 %.UV/Vis: λ_{max}(MeOH) = 581, 406 and 356 nm and λ_{max} (solid, reflectance) = 860, 593 and 378 nm. IR (KBr pellet, cm^{-1}): ν(C=N) 1623 and ν($N(CN)_2^-$) 2180, 2242, 2305.

Synthesis of $^{2}_{\infty}[(NiL)_2Cd(\mu_{1,5}\text{-}N(CN)_2)_2]_n$ (2)

Compound **2** was synthesized in a similar way as **1** but using anhydrous $Cd(ClO_4)_2$ instead of $Ni(ClO_4)_2{\cdot}6H_2O$. The precursor "metalloligand" [NiL] (0.642 g, 2 mmol) was dissolved in methanol (20 mL) and then a water solution (1 mL) of anhydrous $Cd(ClO_4)_2$ (0.311 g, 1mmol) followed by an aqueous solution (1 mL) of sodium dicyanamide (0.180 g, 2 mmol) were added to this solution. The solution was stirred for 1h at room temperature. Here also, a green product separated out during stirring. It was collected by filtration, washed with methanol-water mixture and dried to give **2**. The second crop of **2** as green rhombic shaped X-ray quality single crystals was obtained by the slow evaporation of the filtrate in air. The crystals were washed with methanol-water mixture and dried in a desiccator containing anhydrous $CaCl_2$.

Compound **2**: Yield: 0.785 g, 85% (including the green precipitate and the crystalline compound). Anal. calc. for $C_{38}H_{32}Ni_2N_{10}O_4Cd$: C 49.47, H 3.50, N 15.18 found: C 49.49, H 3.69, N 15.09 %. UV/Vis: λ_{max}(MeOH) = 581, 407 and 360 nm and λ_{max} (solid, reflectance) = 854, 600 and 372 nm. IR (KBr pellet, cm^{-1}): ν(C=N) 1624 and ν($N(CN)_2^-$) 2178, 2240, 2310.

Synthesis of $^{2}_{\infty}[(NiL)_2Zn(\mu_{1,5}\text{-}N(CN)_2)_2]_n$ (3)

Compound **3** was prepared in a similar way as **1** and **2** but using $Zn(ClO_4)_2{\cdot}6H_2O$. The precursor "metalloligand" [NiL] (0.642 g, 2 mmol) was dissolved in methanol (20 mL) and then a water solution (1 mL) of $Zn(ClO_4)_2{\cdot}6H_2O$ (0.372 g, 1 mmol) followed by an aqueous solution (1 mL) of sodium dicyanamide (0.180 g, 2 mmol) were added to this solution. The solution was stirred for 1h at room temperature producing a light blue microcrystalline product that was collected by filtration, washed with methanol-water mixture and dried to furnish **3**. The second crop of **3** as the blue rhombic shaped X-ray quality single crystals was obtained by the slow evaporation of the filtrate in air. The crystals were washed with methanol-water mixture and dried in a desiccator containing anhydrous $CaCl_2$.

Compound **3**: Yield: 0.683 g, 78 % (including the light blue precipitate and the crystalline compound). Anal. calc. for $C_{38}H_{32}Ni_2N_{10}O_4Zn$: C 52.13, H 3.68, N 16.00. found: C 51.96, H 3.91, N 16.16%.UV/Vis: λ_{max}(MeOH) = 583, 406 and 362 nm and λ_{max} (solid, reflectance) = 1026, 566, 420 and 357 nm. IR (KBr pellet, cm^{-1}): ν(C=N) 1624 and ν($N(CN)_2^-$) 2180, 2248, 2323.

Table 1. Crystal data and structure refinement of compounds **1**–**3**

Compounds	1	2	3
Formula	$C_{38}H_{32}Ni_3N_{10}O_4$	$C_{38}H_{32}Ni_2N_{10}O_4Cd$	$C_{38}H_{32}Ni_2N_{10}O_4Zn$
M	868.81	922.53	875.51
Crystal System	Monoclinic	Monoclinic	Orthorhombic
Space Group	$P2_1/c$	$P2_1/c$	Pbcn
a/Å	16.236(5)	16.713(5)	14.9315(7
b/Å	10.705(5)	10.748(5)	19.8367(9)
c/Å	21.821(5)	21.986(5)	12.5335(6)
α/°	90	90	90
β/°	107.244(5)	109.293(5)	90
γ/°	90	90	90
V/Å^3	3622(2)	3728(2)	3712.3(3)
Z	4	4	4
D_c/g cm^{-3}	1.593	1.644	1.566
μ/mm^{-1}	1.601	1.620	1.701
F (000)	1784	1864	1792
R(int)	0.039	0.040	0.038
Total Reflections	52678	33780	40281
Unique reflections	8362	33780	3382
$I>2\sigma(I)$	6531	5899	2757
R1[a], *w*R2[b]	0.0300, 0.0778	0.0311, 0.0855	0.0268, 0.0696
Temp (K)	293	293	293
GOF[c] on F^2	1.02	1.06	1.07

[a]$R1 = \sum||F_o|-|F_c||/\sum|F_o|$, [b]$wR2\ (F_o^2) = [\sum[w(F_o^2 - F_c^2)^2/\sum w\ F_o^4]^{1/2}$ and [c]$GOF = [\sum[w(F_o^2 - F_c^2)^2/(N_{obs} - N_{params})]^{1/2}$

Physical Measurements

Elemental analyses (C, H and N) were performed using a Perkin-Elmer 2400 series II CHN analyzer. IR spectra in KBr pellets (4000-500 cm^{-1}) were recorded using a Perkin-Elmer RXI FT-IR spectrophotometer. Electronic spectra in methanol and in solid state (1200–300 nm) were recorded on a Hitachi U-3501 spectrophotometer. Powder X-ray diffraction patterns were recorded on a Bruker D-8 advance diffractometer operated at 40 kV voltage and 40 mA current and calibrated with a standard silicon sample, using Ni-filtered Cu-Kα (λ = 0.15406 nm) radiation. Magnetic susceptibility measurements were carried out in the temperature range 2-300 K with an applied magnetic field of 0.1 T on polycrystalline samples of **1-3** (with masses of 71.32, 31.33 and 46.76 mg) with a Quantum Design MPMS-XL-5 SQUID susceptometer. The susceptibility data were corrected for the sample holders previously measured using the same conditions and for the diamagnetic contributions of the salt as deduced by using Pascal´s constant tables[12] (χ_{dia} = -440.98x10^{-6}, -452.98x10^{-6} and -443x10^{-6} emu.mol^{-1} for **1**–**3**, respectively).

Crystallographic data collection and refinement

Suitable single crystals of each compound were mounted on a Bruker-AXS SMART APEX II diffractometer equipped with a graphite monochromator and Mo-Kα (λ = 0.71073 Å) radiation. The crystals were positioned at 60 mm from the CCD. Frames (360) were measured with a counting time of 5 s. The structures were solved by Patterson method using the SHELXS 97 program. The non-hydrogen atoms were refined with anisotropic thermal parameters. The hydrogen atoms bonded to carbon were included in geometric positions and given thermal parameters equivalent to 1.2 times those of the atom to which they were attached. Successful convergence was indicated by the maximum shift/error of 0.001 for the last cycle of the least squares refinement. Absorption corrections were carried out using the SADABS program.[13] All the calculations were carried out using SHELXS 97,[14] SHELXL 97,[15] PLATON 99,[16] ORTEP-32[17] and WINGX system ver-1.64.[18] Data collection, structure refinement parameters and crystallographic data for the all three compounds are given in Table 1.

Results and Discussion

Synthesis, IR and UV-Vis spectra of the compounds

The Schiff-base ligand N,N′-bis(salicylidene)-1,3-propanediamine (H_2L) and its corresponding Ni(II) compounds [NiL] was synthesized according to the reported procedure.[11] The [NiL] "metalloligand" on reaction with three different metal(II) (Ni, Cd and Zn) perchlorate salts and sodium dicyanamide, in a 2:1:2 molar ratios in methanol/water medium (10:1, v/v), yielded three 2D CPs $^2_\infty[(NiL)_2Ni(\mu_{1,5}\text{-}N(CN)_2)_2]_n$ (**1**), $^2_\infty[(NiL)_2Cd(\mu_{1,5}\text{-}N(CN)_2)_2]_n$ (**2**) and $^2_\infty[(NiL)_2Zn(\mu_{1,5}\text{-}N(CN)_2)_2]_n$ (**3**) (Scheme 2). All three polymers are constructed by joining of the $[(NiL)_2M]^{2+}$ nodes with the help of dicyanamide spapers. However, the trinuclear nodes are angular in CPs **1** and **2** whereas this is linear in **3** making an interesting difference in the network of the polymer (Scheme2). The phase purity of these three compounds (**1**–**3**) was confirmed by their powder XRD pattern (Fig. S1).

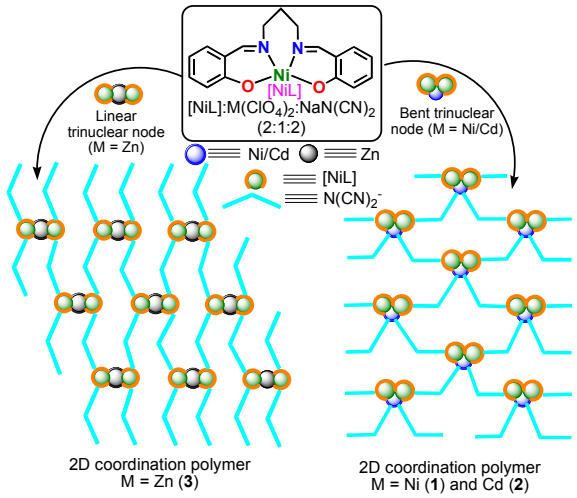

Scheme 2: Construction of 2D coordination polymers.

All three compounds were initially characterized by IR spectroscopy. The precursor "metalloligand" [NiL] does not contain any dicyanamide ion and it is included in the three compounds. The presence of dicyanamido ligands $N(CN)_2^-$ in the compounds is confirmed by the presence of three sharp and strong characteristic stretching frequencies in the 2323–2178 cm^{-1} region. These bands are attributed to $\nu_{as}+\nu_s$(C–N) combination modes, ν_{as}(C≡N) and ν_s(C≡N) vibrations,[19] and are observed at 2305, 2242 and 2180 cm^{-1} in **1**, 2310, 2240 and 2178 cm^{-1} in **2** and 2323, 2248 and 2180 cm^{-1} in **3**. These bands are shifted towards higher frequencies with respect to the free dicyanamide ion that shows the same pattern of bands at 2291, 2231 and 2173 cm^{-1}, indicating the bridging coordination mode of dicyanamide

ion in these three compounds.[20] In addition, a strong and sharp band due to the azomethine ν(C=N) group of the Schiff base appears at 1623, 1624 and 1624 cm^{-1} for compounds **1**–**3**, respectively (Figs. S2–S4). The rest of the spectral pattern and band positions of the respective compounds and "metalloligand" are very similar.

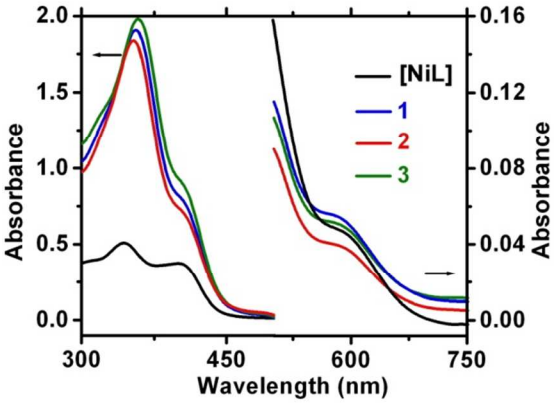

(a)

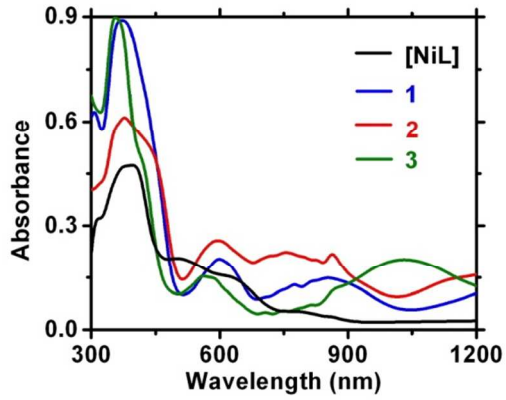

(b)

Fig. 1. The UV-Vis spectra of the compounds (a) in methanolic solution and (b) in solid state.

The UV-Vis spectra of the compounds in methanolic solution and their solid state reflectance spectra are shown in Fig. 1. The electronic spectra of all the compounds in methanol are almost identical but they differ appreciably in the solid state, especially in the visible region. Thus, they show a sharp single absorption band near 356, 360 and 362 nm in methanol and 378, 372 and 357 nm in the solid state for **1**–**3** respectively, attributed to ligand-to-metal charge transfer transitions. Besides this band, a broad absorption band (ν_1) is observed in the visible region at 581, 581 and 583 nm along with a less intense shoulder (ν_2) at 406, 407 and 406 nm in methanol for **1**–**3** respectively, while the "metalloligand" [NiL] shows band maxima (ν_1) at 592 nm along with a less intense shoulder (ν_2) at 406 nm. This band is typical of d–d transitions of Ni(II) ions with a square planar environment. The electronic spectrum for a four coordinate nickel(II) compound with a square planar geometry is expected to exhibit absorption bands near 610 (ν_1) and 500 nm (ν_2) corresponding to the spin allowed d-d transitions $^1B_{1g} \leftarrow {}^1A_g$ and $^1B_{3g} \leftarrow {}^1A_g$ respectively.[21] The observation of the ν_1 and ν_2 bands confirms the square planar environment around Ni(II) in methanol solutions. However, in the solid state, the electronic spectra of **1** and **2** in the visible regions show absorption bands at 593 and 600 nm respectively, which are associated to weaker ones centred at 860 and 854 nm. The electronic spectrum for a five coordinate nickel(II) compound with a square-pyramidal geometry is expected to exhibit absorption bands near 1150 (ν_1), 950 (ν_2), and 600 nm (ν_3), corresponding to the spin allowed d–d transitions $^3T_{2g}(F) \leftarrow {}^3A_{2g}(\nu_1)$, $^3T_{1g}(F) \leftarrow {}^3A_{2g}(\nu_2)$ and $^3T_{1g}(P) \leftarrow {}^3A_{2g}(\nu_3)$, respectively.[22] In the present case, the ν_1 band cannot be located. The observation of the ν_2 and ν_3 bands suggest that the Ni(II) present a square-pyramidal geometry in the solid state. On the other hand, **3** exhibits three distinct bands at 420, 566 and 1026 nm which can be assigned to the spin-allowed d-d transitions $^3T_{1g}(P) \leftarrow {}^3A_{2g}$, $^3T_{1g}(F) \leftarrow {}^3A_{2g}$ and $^3T_{2g}(F) \leftarrow {}^3A_{2g}$ respectively. These values agree with the literature values for octahedral Ni(II) compounds.[23] Thus the spectral data in solid state agrees with the X-ray structural data (see below).

Structure description of the compounds

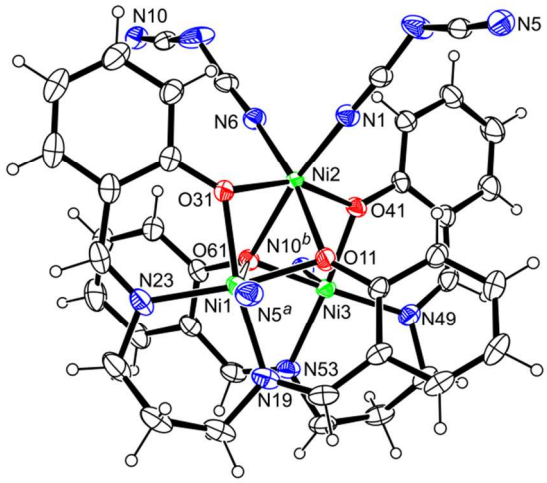

Fig. 2. The coordination environment of metal ions in the trinuclear unit of compound of **1** with ellipsoids at 30% probability (Symmetry transformation [a] = -x, -1/2+y, 1/2-z and [b] = 1-x, -1/2+y, 1/2-z). The weak Ni1–O61 bond is shown by an open bond.

The structure of **1** is depicted in Fig. 2 together with the atomic numbering scheme. Bond parameters within the metal coordination spheres are given in Table 2. The neutral trinuclear entity of this compound $[(NiL)_2Ni(\mu_{1,5}\text{-}N(CN)_2)_2]$ contains two [NiL] "metalloligands" (where H_2L is N,N'-bis(salicylidene)-1,3-propanediamine), one Ni(II) ion and two $\mu_{1,5}$-dicyanamido (dca^-) moieties. The Ni(II) ions of the [NiL] units (Ni1 and Ni3) present a penta-coordinated square pyramidal geometry (Ni1 could also be viewed as an elongated octahedron if we consider the weak Ni1–O61 bond distance of 2.441(6) Å). The basal planes around these nickel atoms are constituted by the two imine nitrogen atoms and two phenoxido oxygen atoms from the tetradentate Schiff base ligand. The axial positions of both nickel atoms are occupied by the terminal nitrogen atoms of dca^- ligands. The basal and axial Ni–O and Ni–N bond distances in both nickel atoms are very similar (Table 2). The four donor atoms in the equatorial plane show r.m.s. (root mean squared) deviations of

0.071 and 0.083 Å for Ni1 and Ni3 respectively. The metal atoms are shifted by 0.119(1) and 0.191(1) Å, respectively, from their mean plane towards the axially coordinated nitrogen atoms. The Addison parameters (τ = 0.047 for Ni1 and 0.119 for Ni3) indicate that distortion towards trigonal bipyramid is negligible for both metal atoms ($\tau = 0$ for the ideal square pyramid and $\tau = 1$ for the trigonal bipyramid[24]). The dihedral angle between the two N_2–Ni–O_2 planes is 15.78(9)° indicating that the two "metalloligands" are almost parallel to each other.

The central Ni2 atom has an octahedral environment formed by four oxygen atoms from the two chelating "metalloligands" and by two terminal *cis*-dca$^-$ ligands with very similar bond lengths (Table 2). The *cis* [73.62(6) –98.63(7)°] and the *trans* [156.98(5) –170.61(7)°] angles indicate significant distortions from ideal octahedral geometry. The Ni1···Ni2, Ni2···Ni3 and Ni3···Ni1 distances are 2.938(2), 3.033(2) and 3.746(2) Å, respectively. The Ni1–Ni2–Ni3 angle is 77.72(1)° indicating a bent arrangement of the metal atoms in the Ni_3 unit.

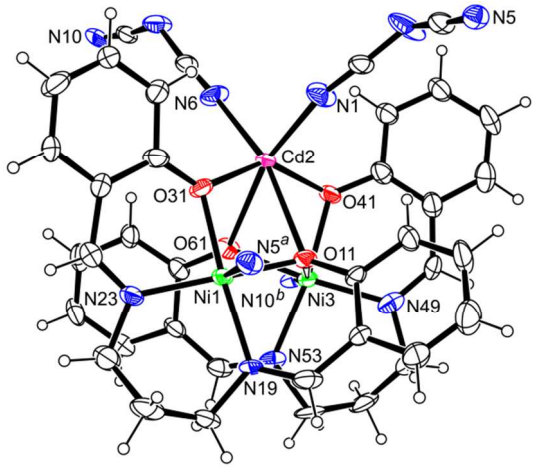

Fig. 3. The coordination environment of metal ions in the trinuclear unit of compound **2** with ellipsoids at 30% probability (symmetry transformations [a] = 2-x,-1/2+y,3/2-z and [b] =1-x,-1/2+y,3/2-z). The weak Ni3–O11 bond is shown by an open bond.

Compound **2** is isostructural to **1** but with a central Cd(II) ion instead of a Ni(II) (Fig. 3), thus forming a neutral trinuclear unit of formula $[(NiL)_2Cd(\mu_{1,5}\text{-}N(CN)_2)_2]$. As expected, a comparison of the bond lengths and angles between **1** and **2** shows very small differences (Table 2). The r.m.s. deviations of the coordinated atoms in the basal planes are 0.103 and 0.102 Å around Ni1 and Ni3, respectively. The metal atoms are 0.142(2) and 0.077(2) Å from their mean planes. The Addisson parameters (0.140 for Ni1 and 0.058 for Ni3) also confirm a slightly distorted square pyramidal geometry around the metal centers.

As observed in **1**, the geometry around Ni3 may be viewed as a distorted elongated octahedral with an elongated Ni3–O11 bond distance of 2.363(2) Å and an axial *trans* angle of 164.54(10)°. The two "metalloligands" are also nearly parallel to each other as indicated by the dihedral angle (13.9(5)°) between the two N_2–Ni–O_2 planes. The cadmium atom, Cd(2) has a similar distorted octahedral environment to Ni(2) as in compound **1**. The *cis* [63.92(9)–106.19(10)°] and *trans* [142.48(7)–164.89(9)°] angles also indicate significant distortions from the ideal octahedral geometry around the cadmium atom. The Cd···Ni distances are 3.269(2) and 3.162(3) Å whereas the Ni···Ni distance is 3.668(3) Å. Like in **1**, the Ni1–Cd2–Ni3 angle (69.53(3)°) indicates an extremely bent arrangement of the three metal atoms in the Ni_2Cd unit.

Table 2. Bond distances (Å) and angles (°) for compounds **1** and **2**.

	Compound **1**	Compound **2**
Ni(1)–O(11)	1.9813(18)	2.033(2)
Ni (1)–O(31)	2.0036(17)	1.982(2)
Ni (1)–N(19)	2.039(2)	2.043(2)
Ni (1)–N(23)	2.014(2)	2.031(3)
Ni (1)–N(5)[a]	2.087(2)	2.038(3)
Ni(2)/Cd(2)–O(11)	2.086(2)	2.531(2)
Ni(2)/Cd(2)–O(31)	2.0532(16)	2.190(2)
Ni(2)/Cd(2)–O(41)	2.0192(16)	2.215(2)
Ni(2)/Cd(2)–O(61)	2.1966(18)	2.362(3)
Cd(2)/Ni(2)–N(1)	2.032(2)	2.246(3)
Ni(2)/Cd(2)–N(6)	2.026(2)	2.242(3)
Ni(3)–O(41)	1.9778(16)	2.023(2)
Ni(3)–O(61)	2.0199(17)	2.001(3)
Ni(3)–N(49)	2.014(2)	2.033(3)
Ni(3)–N(53)	2.028(2)	2.056(2)
Ni(3)–N(10)[b]	2.036(2)	2.090(3)
O(11)–Ni(1)–O(31)	80.92(6)	88.70(8)
O(11)–Ni(1)–N(19)	89.04(8)	86.57(9)
O(11)–Ni(1)–N(23)	166.96(8)	166.29(10)
O(11)–Ni(1)–N(5)[a]	95.01(8)	95.83(10)
O(31)–Ni(1)–N(19)	169.80(7)	174.73(9)
O(31)–Ni(1)-N(23)	91.74(7)	88.34(8)
O(31)–Ni(1)–N(5)[a]	95.86(7)	92.04(9)
N(19)–Ni(1)–N(23)	97.78(9)	95.72(10)
N(19)–Ni(1)–N(5)[a]	86.71(8)	90.76(10)
N(23)–Ni(1)–N(5)[a]	96.47(8)	97.65(11)
O(11)–Ni(2)/Cd(2)–O(31)	77.31(6)	72.56(7)
O(11)–Ni(2)/Cd(2)–O(41)	84.93(6)	74.08(7)
O(11)–Ni(2)/Cd(2)–O(61)	73.62(6)	63.92(9)
O(11)–Ni(2)/Cd(2)–N(1)	97.13(7)	98.27(9)
O(11)–Ni(2)/Cd(2)–N(6)	169.97(7)	164.89(9)
O(31)–Ni(2)/Cd(2)–O(41)	156.98(5)	142.48(7)
O(31)–Ni(2)/Cd(2)–O(61)	81.52(6)	77.79(9)
O(31)–Ni(2)/Cd(2)–N(1)	98.27(7)	99.19(10)
O(31)–Ni(2)/Cd(2)–N(6)	98.63(7)	101.65(10)
O(41)–Ni(2)/Cd(2)–O(61)	79.47(5)	72.45(8)
O(41)–Ni(2)/Cd(2)–N(1)	98.38(7)	102.13(10)
O(41)–Ni(2)/Cd(2)–N(6)	96.42(7)	106.19(10)
O(61)–Ni(2)/Cd(2)–N(1)	170.61(7)	162.11(11)
O(61)–Ni(2)/Cd(2)–N(6)	96.81(7)	101.46(11)
N(1)–Ni(2)/Cd(2)–N(6)	92.51(8)	96.43(11)
O(41)– Ni(3)–O(61)	84.90(5)	84.60(11)
O(41)– Ni(3)–N(49)	89.52(6)	90.66(11)
O(41)– Ni(3)–N(53)	170.76(7)	172.23(9)
O(41)– Ni(3)–N(10)[b]	94.76(7)	91.33(11)
O(61)– Ni(3)–N(49)	163.64(7)	168.78(12)
O(61)– Ni(3)-N(53)	87.46(7)	88.20(12)
O(61)– Ni(3)–N(10)[b]	96.47(7)	93.46(12)
N(49)– Ni(3)–N(53)	96.43(7)	96.94(12)
N(49)– Ni(3)–N(10)[b]	99.31(8)	96.81(12)
N(53)– Ni(3)–N(10)[b]	91.25(8)	86.20(12)

Symmetry transformation [a] = -x,-1/2+y,1/2-z and [b] = 1-x,-1/2+y,1/2-z for **1** and [a] = 2-x,-1/2+y,3/2-z and [b] =1-x,-1/2+y,3/2-z for **2**.

The trinuclear nodes in both compounds **1** and **2** are angular with Ni–Ni–Ni or Ni–Cd–Ni angles of 77.72(1) or 69.53(3)º, respectively. In both compounds, the two dicyanamido bridges present a V-shaped geometry with NC–N–CN angles of 122.1(2) and 123.6(2)º in **1** and 123.30(1) and 121.83(1)º in **2**, and occupy two *cis* positions of the octahedral coordination sphere of the central Ni2 or Cd2 atom. These two dca$^-$ bridges connect each

trinuclear unit with the terminal Ni centres of two different neighbouring trinuclear units. As a result, each trinuclear Ni_3 or Ni_2Cd is connected with four neighbouring trinuclear units: with two of them acting as dca-donor and with the other two as dca-acceptor. This connectivity results in square 2D coordination networks for both compounds (Fig. 4a for **1** and Fig. S5 in SI for **2**). The topological analysis of this network can be simplified by considering the centroid of the trinuclear $[(NiL)_2M]^{2+}$ units (M = Ni for **1** and Cd for **2**) as 4-connected cluster nodes. This uninodal 4-connected net features the **sql** (Shubnikov tetragonal plane net) topology with the point symbol of $(4^4.6^2)$.

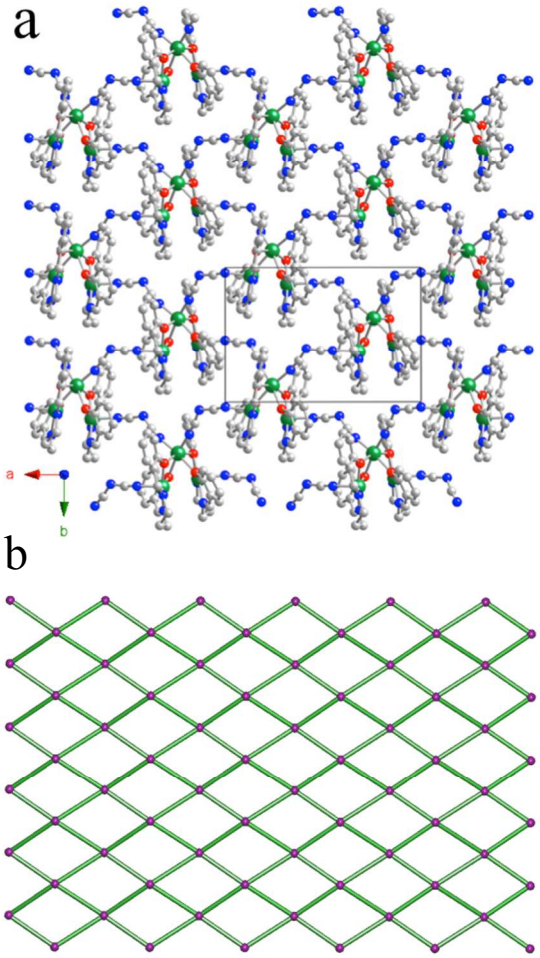

Fig. 4. (a) The 2D coordination newtork in **1** constructed by assembling in the trinuclear $[(NiL)_2Ni]^{2+}$ units through the central and terminal Ni centres with the dca^- bridges. All H atoms are omitted for clarity, Ni = green, N = blue, O = red, C = grey. (b) Simplified uninodal 4-connected net with the **sql** topology and the point symbol of $(4^4.6^2)$. Centroids of the 4-connected trinuclear units are shown as violet balls.

Compound **3** contains neutral trinuclear units of formula $[(NiL)_2Zn(\mu_{1,5}\text{-}N(CN)_2)_2]$ presenting a crystallographic 2-fold axis passing through the central Zn atom (Fig. 5). In this trinuclear unit, the three metal atoms (two terminal Ni atoms and the central Zn atom) are almost co-linear, in clear contrast to the observed bent geometry in the trinuclear unit **1** and **2**. The two equivalent terminal Ni(II) ions present an elongated octahedral geometry where the basal plane is formed by the two imine nitrogen atoms and two phenoxido oxygen atoms from one ‘‘metalloligand”. These four donors in the equatorial plane show r.m.s. deviation from their mean plane around the Ni center of 0.081 Å while the metal atom deviates 0.004(1) Å from this plane in the direction of the N1 atom. The basal Ni-O and Ni-N bond distances are very similar (Table 3). The apical positions are occupied by the terminal nitrogen atoms from two dicyanamido ligands. The apical Ni–N bond lengths are slightly longer than the basal Ni–N ones. The axial *trans* angle (177.62(8)º) is close to 180°. In contrast to **1** and **2**, the dihedral angle between the two N_2–Ni–O_2 planes is 67.65(18)° indicating that the two “metalloligands” are almost perpendicular (Fig. 5).

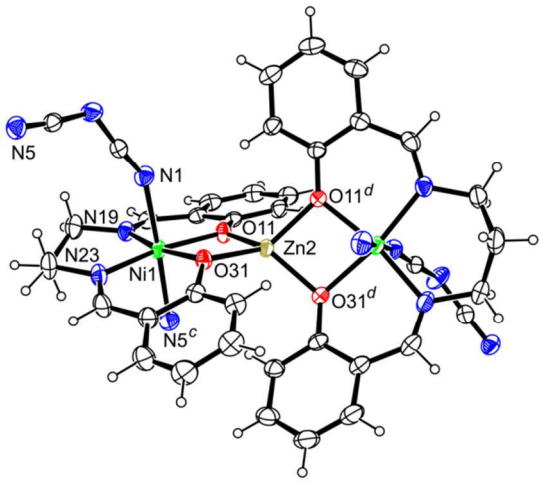

Fig. 5. The coordination environment of the metal ions in the structure of compound **3** with ellipsoids at 30% probability (symmetry [c] = 1/2+x,1/2-y,2-z and [d] = -x,y,3/2-z).

Table 3. Bond distances (Å) and angles (°) for compound **3**.

Ni(1)–O(11)	2.0306(15)	O(31)–Ni(1)–N(19)	169.00(7)
Ni(1)–O(31)	2.0566(15)	O(31)–Ni(1)–N(23)	90.75(7)
Ni(1)–N(19)	2.0198(19)	O(31)–Ni(1)–N(5)^c	92.75(7)
Ni(1)–N(23)	2.020(2)	N(1)–Ni(1)–N(19)	88.30(8)
Ni(1)–N(1)	2.139(2)	N(1)–Ni(1)–N(23)	90.41(8)
Ni(1)–N(5)^c	2.120(2)	N(1)–Ni(1)–N(5)^c	177.62(8)
Zn(1)–O(11)	1.9462(15)	N(19)–Ni(1)–N(23)	99.56(8)
Zn(1)–O(31)	1.9538(15)	N(19)–Ni(1)–N(5)^c	91.59(8)
O(11)–Ni(1)–O(31)	79.40(6)	N(23)–Ni(1)–N(5)^c	87.27(8)
O(11)–Ni(1)–N(1)	94.33(7)	O(11)–Zn(1)–O(31)	84.05(6)
O(11)–Ni(1)–N(19)	90.65(7)	O(11)–Zn(1)–O(11)^d	112.26(7)
O(11)–Ni(1)–N(23)	168.87(8)	O(11)–Zn(1)–O(31)^d	131.45(6)
O(11)–Ni(1)–N(5)^c	88.05(7)	O(31)–Zn(1)–O(31)^d	119.89(6)
O(31)–Ni(1)–N(1)	87.79(7)		

Symmetry transformation [c] = 1/2+x,1/2-y,2-z and [d] = -x,y,3/2-z for **3**.

Another remarkable difference between **1**–**2** and **3** is the tetrahedral environment of the Zn(II) ion which is bonded to four bridging phenoxido oxygen atoms from two different [NiL] units. The Zn–O bonds lengths are very similar (1.9462(15) and 1.9538(15) Å) forming a distorted-tetrahedron with O–Zn–O bond angles in the range 84.05(6)–131.45(6)º (Table 3). The distorted tetrahedral geometry around the Zn(II) ion is suggested by the dihedral angle of 75.37(14)º between the two O–Zn–O planes (the dihedral angle is 0º for a perfectly square planar arrangement and 90º for a perfect tetrahedral arrangement) and confirmed by its τ_4 index of 0.77. The τ_4 index is defined as $\tau_4 = [360º - (\alpha + \beta)]/141º$, with α and β (in º) being the two largest

angles around the central metal in the compound with $\tau_4 = 0$ for a perfect square planar and $\tau_4 = 1$ for a perfect tetrahedron.[25] The Ni1···Zn2 and Ni1···Ni1 distances are 3.016(1) and 6.032 Å respectively. The Ni1–Zn2–Ni3 angle is 179.22(1)°.

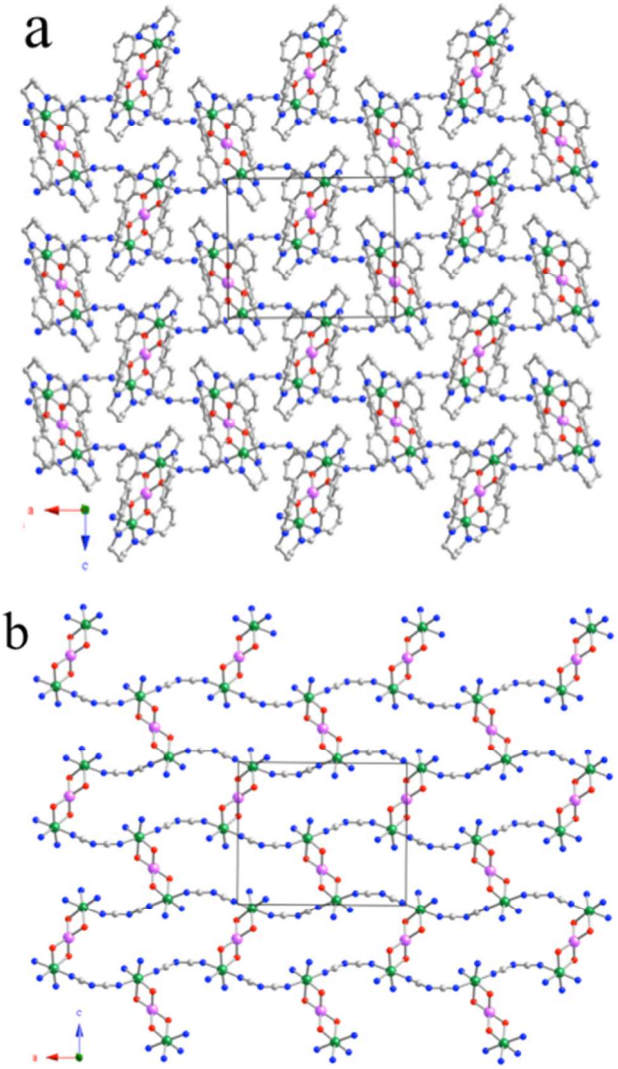

Fig. 6. (a) The 2D coordination newtork in **3** constructed by assembling of the trinuclear $[(NiL)_2Zn]^{2+}$ units through only terminal Ni centres with the help of $\mu_{1,5}$-dicyanamido linkers. All H atoms are omitted for clarity. (b) Simplified view of the eclipsed layers stacking in the ··AA·· fashion (only the bridging ligands and the coordinating sphere of the metals are drawn). Ni = green, Zn = pink, N = blue, O = red and C = grey.

The connectivity of the trinuclear units in **3** is established through V-shaped dicyanamido bridges with NC–N–CN angles of 119.9(2)º (close to those observed in **1** and **2**). However, these dca$^-$ bridges occupy *trans* positions in the two terminal Ni atoms, giving rise to a corrugated topology where each Ni_2Zn is connected to four different Ni_2Zn trinuclear units through single $\mu_{1,5}$-dicyanamido bridges between only terminal nickel centers (Fig. 6a). These layers stack in an eclipsed way along the *b* axis (Fig. 6b). The topological analysis of this structure in **3** assuming the centroid atom of the trinuclear unit is the same uninodal 4-connected net observed in **1** and **2**: Shubnikov tetragonal plane net topology with the point symbol of $(4^4.6^2)$ (Fig. 4b).

Magnetic properties

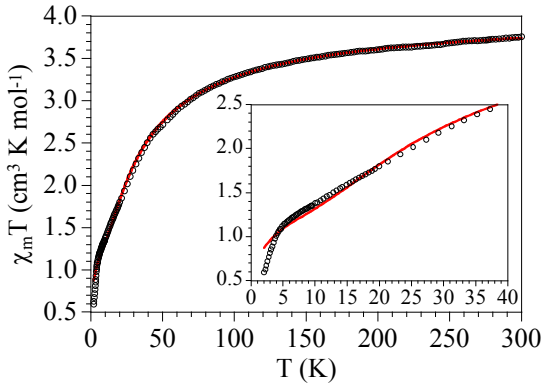

Fig. 7. Thermal variation of $\chi_m T$ for compound **1**. Solid line is the best fit to the model (see text). Inset shows the low temperature region.

Compound **1** shows at room temperature a $\chi_m T$ value of ca. 3.5 cm^3 K mol^{-1} (χ_m is the magnetic susceptibility per Ni_3 trinuclear unit), which is the expected value for three isolated Ni(II) S = 1 ions (Fig. 7). When the sample is cooled, $\chi_m T$ shows a progressive decrease with a smoothening of the slope between 10 and 5 K where the $\chi_m T$ value is ca. 1.2 cm^3 K mol^{-1} (inset in Fig. 7). This value is the expected one for a S = 1 spin state. Below ca. 5 K $\chi_m T$ shows a more abrupt decrease reaching a value of ca. 0.6 cm^3 K mol^{-1} at 2 K (inset in Fig. 7). This result indicates that the three Ni(II) ions in **1** present an antiferromagnetic coupling that results in a S = 1 spin ground state for the trinuclear unit. At very low temperatures this spin state presents a zero field splitting (ZFS) and/or inter-trinuclear antiferromagnetic interactions, through the single dca$^-$ bridges, responsible for the abrupt decrease below ca. 5 K. Although the structure of the Ni_3 compound show that it is a bent trinuclear unit, in fact, it can be considered as a linear trinuclear unit from the magnetic point of view since there are no direct bridges connecting the two terminal Ni atoms (if we neglect the long Ni1–O61 bond distance of 2.441(6) Å). Since the central Ni2 atom is connected with the two terminal Ni1 and Ni3 atoms through similar double phenoxido bridges, we can consider, in a first approach, that compound **1** is a linear symmetric trinuclear unit with only one intra-trinuclear coupling constant (J). Finally, to account for the possible inter-trinuclear interactions through the single dca$^-$ bridges, we have included an inter-trinuclear term using the molecular field approximation. Accordingly, we have fit the magnetic properties of **1** to a linear centrosymmetric S = 1 trinuclear model (J) with inter-trinuclear interactions (zj) and a paramagnetic monomeric S = 1 impurity (c) to account for possible monomeric impurities and vacant compounds. This model reproduces very satisfactorily the magnetic properties of compound **1** in the 5-300 K temperature range with the following parameters: g = 2.127, J = -12.9 cm^{-1}, zj = -0.4 cm^{-1} and c = 5.9 % (the Hamiltonian is written as $H = -JS_iS_{i+1}$). At very low temperatures (below 5 K) the fit is not good because we have not included a ZFS of the resulting S = 1 spin state since both parameters (ZFS and inter-trinuclear coupling) are similar in magnitude and are strongly correlated, precluding a precise determination of them. Note also that, although the two J values are not equivalent by symmetry,

they must be very similar, as demonstrated by the good agreement between the experimental and theoretical values. The antiferromagnetic coupling in the linear trinuclear unit leads to a S = 1 ground spin state as confirmed by the isothermal magnetization at 2 K that shows a saturation value close to 2.0μ_B, the expected value for a S = 1 spin state with g ≈ 2 (Fig. S6).

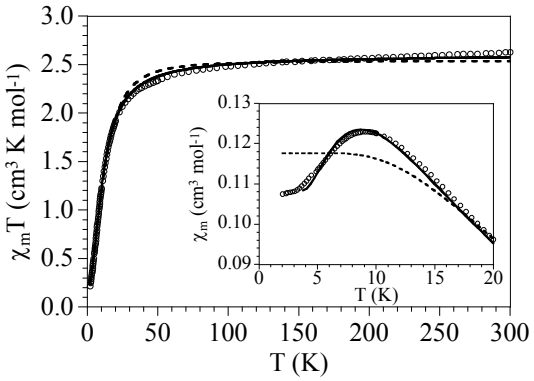

Fig. 8. Thermal variation of $\chi_m T$ for compound **2**. Solid and dashed lines are the best fit to the dimer and monomer S = 1 models, respectively. Inset shows the low temperature region of the thermal variation of χ_m.

Compound **2** shows at room temperature a $\chi_m T$ value of ca. 2.5 cm^3 K mol^{-1} per Ni_2Cd trinuclear unit, the expected value for two isolated Ni(II) S = 1 ions (Fig. 8). When the sample is cooled, $\chi_m T$ remains constant down to ca. 50 K and below this temperature it shows a progressive decrease to reach a value of ca. 0.2 cm^3 K mol^{-1} at 2 K. This behaviour indicates the presence of very weak antiferromagnetic interactions between the two Ni ions in **2**. Since the central Cd(II) ion is diamagnetic, the Ni(II) ions are magnetically quite well isolated, except for the presence of weak Ni–O bonds, connecting both terminal Ni(II) ions in the trinuclear unit. Therefore, we can assume that the decrease observed at low temperature may arise from a weak antiferromagnetic coupling between the two Ni ions through weak Ni–O–Ni bridges and/or from the ZFS of the Ni(II) ions. Accordingly, we have used two different models to fit the magnetic properties: (1) a S = 1 monomer with ZFS and (2) a S = 1 dimer with ZFS. The first model reproduces quite satisfactorily the magnetic data with the following parameters: g = 2.254 and |D| = 29.5 cm^{-1} (dashed line in Fig. 8). The second model reproduces even better the magnetic data, especially at low temperatures, with g = 2.187, J = -2.4 $cm^{-1}$and |D| = 14.8 cm^{-1} (solid line in Fig. 8, the Hamiltonian is written as $H = -JS_1S_2$). Although it could be argued that the better agreement is due to the use of an additional fitting parameter (J), the presence of a weak intra-trinuclear antiferromagnetic Ni···Ni interaction is confirmed by the presence of a maximum in the χ_m plot at ca. 10 K (inset in Fig. 8). As expected, only the dimer model is able to reproduce satisfactorily this maximum. A limit in the used model is the fact that the D and J values are strongly correlated, precluding a reliable determination of them. In fact, the D value obtained is quite high. Note also that we have not considered any inter-trinuclear interaction because the single dca^- bridges connecting the trinuclear units always link a Ni(II) with a Cd(II) ion. Finally, the isothermal magnetization confirms the presence of the antiferromagnetic coupling and shows an almost linear behaviour without reaching saturation even at 5 T (Fig. S7).

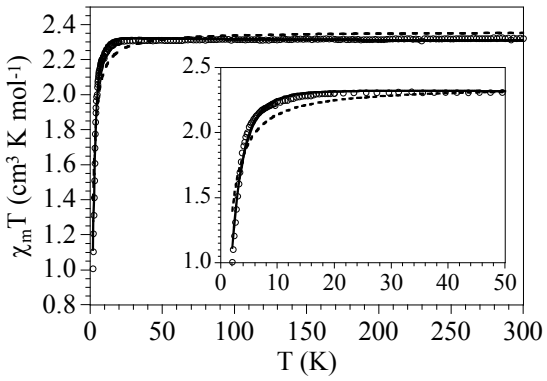

Fig. 9. Thermal variation of $\chi_m T$ for compound **3**. Solid and dashed lines are the best fit to the S = 1 regular chain model with D < 0 or D > 0, respectively. Inset shows the low temperature region.

Compound **3** shows at room temperature a $\chi_m T$ value of ca. 2.3 cm^3 K mol^{-1} per Ni_2Zn trinuclear unit, the expected value for two isolated Ni(II) S = 1 ions (Fig. 9). On cooling down the sample, $\chi_m T$ remains constant down to ca. 10 K. Below this temperature $\chi_m T$ shows a progressive decrease to reach a value of ca. 1.0 cm^3 K mol^{-1} at 2 K. Since the Zn(II) ions is diamagnetic, we can consider that the only possible exchange pathway is the one taking place through the dca^- single bridges connecting the Ni_2Zn trinuclear units. This exchange pathway gives rise to regular Ni(II) chains as clearly shown in Fig. 6b. Accordingly, we have fit the magnetic data of **3** to a regular S = 1 chain model with ZFS.[26] Since, a priori we do not know the sign of D, we have used both models (for D positive and D negative). As can be clearly observed in Fig. 9, the model with positive D (g = 2.172, J = -0.47 cm^{-1} and D = 0.8 cm^{-1}, dashed line in Fig. 9, the Hamiltonian is written as $H = -JS_iS_{i+1}$) gives a poorer agreement than the model with negative D (g = 2.148, J = -0.44 cm^{-1} and D = - 3.9 cm^{-1}, solid line in Fig. 9) and, accordingly, we can assume that compound **3** presents a negative D value. The very weak antiferromagnetic coupling is also confirmed by the isothermal magnetization at 2 K that shows a saturation value close to 2.3 μ_B, the expected one for a S = 1 ion with g = 2.15 (Fig. S8).

The weak antiferromagnetic coupling found in compound **1** is surprising since previous magneto-structural correlations in similar double oxido bridged Ni(II) clusters indicate that the coupling is expected to be ferromagnetic when the Ni–O–Ni bond angle is in the range 90-98º.[27] In compound **1** the Ni–O–Ni bond angles are in the range 91.88–98.70º with average values of 92.60º and 95.29º for the Ni1···Ni2 and Ni2···Ni3 couplings, respectively. Albeit, the dihedral Ni–O–O–Ni angle also plays an important role.[28] In compound **1** these dihedral angles are far from 180º (these are 139.35º for Ni1–O11–O31–Ni2 and 157.38º for Ni2–O41–O61–Ni3) and, therefore, the magnetic coupling is expected to be weak and antiferromagnetic, as observed experimentally. In compound **2** the weak antiferromagnetic coupling found (J = -2.4 cm^{-1}) is not surprising since the two Ni(II) ions are bridged by a double asymmetric phenoxido bridge. One of them (Ni3–O11 has one long distance of 2.363(2) Å and a Ni1–O11–Ni3 large bond angle of 112.89(1)º, which is expected

to give rise to a weak antiferromagnetic coupling). The second bridge can be neglected since it present a very long Ni1–O61 bond distance of 2.81(1) Å and a Ni1–O61–Ni3 bond angle close to the crossing point between ferro- and antiferro-magnetic coupling (97.96(2)º). In compound **3** the very weak antiferromagnetic coupling found (J = -0.44 cm^{-1}) has to be attributed to the long NC–N–CN^- inter-trinuclear bridge since there is no Ni···Ni intra-trinuclear interactions. This ligand is very well known to give rise to weak antiferromagnetic interactions, in agreement[29] with the result found in compound **3**.

Conclusions

In this paper, using trinuclear $\{[NiL]_2M\}^{2+}$ nodes derived from an acyclic tetradentate N_2O_2 type Schiff base and dicyanamide spacers we synthesized three 2D CPs having different networks. Among them, the isomorphous compounds **1** and **2** are constructed by linking of bent trinuclear nodes $\{[NiL]_2M\}^{2+}$ (M = Ni for **1** and Cd for **2**) *via* $\mu_{1,5}$-bridging dicyanamido spacers through the central Ni or Cd of one node to terminal Ni centres of two different nodes. In contrast, the unique 2D CP of **3** are resulted from linear trinuclear nodes $\{[NiL]_2Zn\}^{2+}$ which are connected by $\mu_{1,5}$-bridging dicyanamide spacers through terminal Ni centres of neighbouring nodes. The different shapes of the trinuclear nodes are originated due to the different coordination environment of the central metal ions. The octahedral environment of Ni or Cd in **1** or **2** results bent nodes in which the two [NiL] "metalloligands" are almost parallel to each other. On the other hand, in **3**, Zn is tetrahedrally coordinated making the two [NiL] "metalloligands" nearly perpendicular in linear disposition. The presence of different central hetero-metal ions into the trinuclear nodes brings about significant variation in the magnetic properties of the CPs. In **1** the intra-trinuclear interactions between the three phenoxido bridged Ni(II) ions are moderate antiferromagnetic, whereas in **2** the weak antiferromagnetic intra-trinuclear interaction is only between the two terminals Ni(II). The very weak inter-trinuclear antiferromagnetic interactions between Ni(II) is through the single $\mu_{1,5}$-bridging dicyanamide spacer in **3**. The present system thus reveals that the central metal ion in this kind of trinuclear nodes is important in determining the final network of the CP and their magnetic interactions. Therefore, different trinuclear nodes can potentially be explored in future studies of CPs, namely towards the design of novel metal–organic materials with diverse topologies and functional properties by changing metal ions.

Acknowledgements

L. K. D. is thankful to CSIR, India for awarding Senior Research Fellowship [Sanction No. 09/028 (0805)/2010-EMR-I]. The authors also thank the Department of Science and Technology (DST), New Delhi, India, for financial support (SR/S1/IC/0034/2012). Crystallography was performed at the DST-FIST; India funded Single Crystal Diffractometer Facility at the Department of Chemistry, University of Calcutta. We also thank the Spanish MINECO (CTQ-2011-26507) and the Generalitat Valenciana (Prometeo and ISIC-Nano programs) for financial support.

Notes and references

[a]Department of Chemistry, University College of Science and Technology, University of Calcutta, 92, A.P.C. Road, Kolkata-700 009, India; e-mail: ghosh_59@yahoo.com
[b]Instituto de Ciencia Molecular (ICMol), Universidad de Valencia. C/Catedrático José Beltrán, 2. 46980 Paterna, Valencia, Spain.

†Electronic Supplementary Information (ESI) available Experimental and simulated X-ray powder diffractograms of the three compounds (Fig. S1), IR spectra of the three compounds (Figs. S2–S4), 2D coordination network for compound **2** (Fig. S5) and isothermal magnetization of the three compounds (Figs. S6–S8) are included as supporting information. CCDC 1022779-1022781 contain the supplementary crystallographic data in CIF format for **1-3** respectively. These data can be obtained free of charge via http://www.ccdc.cam.ac.uk/conts/retrieving.html, or from the Cambridge Crystallographic Data Centre, 12 Union Road, Cambridge CB2 1EZ, UK; fax: (+44) 1223-336-033; or e-mail: deposit@ccdc.cam.ac.uk. See DOI: 10.1039/b000000x/.

1 (*a*) T. Yamada, K. Otsubo, R. Makiura and H. Kitagawa, *Chem. Soc. Rev.*, 2013, **42**, 6655–7044; (*b*) O. Kahn, J. Larionova and L. Ouahab, *Chem. Commun.*, 1999, 945–952; (*c*) M. J. Zaworotko, *Chem. Commun.*, 2001, 1–9; (*d*) B. Moulton and M. J. Zaworotko, *Chem. Rev.*, 2001, **101**, 1629–1658; (*e*) M. Du, C.-P. Li, C.-S. Liu and S.-M. Fang, *Coord. Chem. Rev.*, 2013, **257**, 1282–1305; (*f*) C. Janiak, *Dalton Trans.*, 2003, 2781–2804; (*g*) S. L. James, *Chem. Soc. Rev.*, 2003, **32**, 276–288; (*h*) K. Biradha, M. Sarkar and L. Rajput, *Chem. Commun.*, 2006, 4169–4179; (*i*) Y.-Y. Liu, Y.-Y. Jiang, J. Yang, Y.-Y. Liu and J.-F. Ma, *CrystEngComm*, 2011, **13**, 6118–6129; (*j*) J.-P. Zhang, X.-C. Huang and X.-M. Chen, *Chem. Soc. Rev.*, 2009, **38**, 2385–2396; (*k*) A. Y. Robin and K. M. Fromm, *Coord. Chem. Rev.*, 2006, **250**, 2127–2157; (*l*) A. Erxleben, *Coord. Chem. Rev.*, 2003, **246**, 203–228.

2 (*a*) C. Janiak and J. K. Vieth, *New J. Chem.*, 2010, **34**, 2366–2388; (*b*) N. N. Adarsh and P. Dastidar, *Chem. Soc. Rev.*, 2012, **41**, 3039–3060.

3 (*a*) R. W. Gable, B. F. Hoskins and R. Robson, *J. Chem. Soc., Chem. Commun.*, 1990, 1677–1678; (*b*) B. F. Hoskins and R. Robson, *J. Am. Chem. Soc.*, 1990, **112**, 1546–1554.

4 M. Andruh, *Chem. Commun.*, 2007, 2565–2577.

5 (*a*) L. K. Das and A. Ghosh, *CrystEngComm*, 2013, **15**, 9444–9456; (*b*) L. K. Das, A. M. Kirillov and A. Ghosh, *CrystEngComm*, 2014, **16**, 3029–3039.

6 (*a*) S. Ghosh, S. Mukherjee, P. Seth, P. S. Mukherjee and A. Ghosh, *Dalton Trans.*, 2013, **42**, 13554–13564; (b) S. Biswas, C. J. Gómez-García, J. M. Clemente-Juan, S. Benmansour, and A. Ghosh, *Inorg. Chem.* 2014, **53**, 2441−2449.

7 S. Ghosh, Y. Ida, T. Ishida and A. Ghosh, *Cryst. Growth Des.*, 2014, **14**, 2588−2598.

8 (*a*) M. Andruh, *Pure Appl. Chem.*, 2005, **77**, 1685–1706; (*b*) M. Andruh, D. G. Branzea, R. Gheorghe and A. M. Madalan, *CrystEngComm*, 2009, **11**, 2571–2584.

9 (*a*) A. M. Madalan, H. W. Roesky, M. Andruh, M. Noltemeyer and N. Stanica, *Chem. Commun.*, 2002, 1638–1639; (*b*) J.-P. Costes, R. Gheorghe, F. Dahan, M. Andruh, S. Shova and J.-M. Clemente Juan, *New J. Chem.*, 2006, **30**, 572–576; (*c*) D. G.

Branzea, A. Guerri, O. Fabelo, C. Ruiz-Pérez, L.-M. Chamoreau, C. Sangregorio, A. Caneschi and M. Andruh, *Cryst. Growth Des.*, 2008, **8**, 941–949; (*d*) D. Visinescu, A. M. Madalan, M. Andruh, C. Duhayon, J.-P. Sutter, L. Ungur, W. V. Heuvel and L. F. Chibotaru, *Chem.–Eur. J.*, 2009, **15**, 11808–11814; (*e*) R. Gheorghe, A. M. Madalan, J.-P. Costes, W. Wernsdorferd and M. Andruh, *Dalton Trans.*, 2010, **39**, 4734–4736.

10 (*a*) M. Andruh, *Chem. Commun.*, 2011, **47**, 3025–3042; (*b*) D. G. Branzea, A. M. Madalan, S. Ciattini, N. Avarvari, A. Caneschi and M. Andruh, *New J. Chem.*, 2010, **34**, 2479–2490.

11 O. Atakol, H. Nazir, C. Arici, S. Durmus, I. Svoboda and H. Fuess, *Inorg. Chim. Acta*, 2003, **342**, 295−300.

12 G. A. Bain and J. F. Berry, *J. Chem. Educ.*, 2008, **85**, 532−536.

13 SAINT, version 6.02; SADABS, version 2.03, Bruker AXS, Inc., Madison, WI, 2002.

14 G. M. Sheldrick, *SHELXS 97*, *Program for Structure Solution*, University of Göttingen, Germany, 1997.

15 G. M. Sheldrick, *SHELXL 97*, *Program for Crystal Structure Refinement*, University of Göttingen, Germany, 1997.

16 A. L. Spek, PLATON. Molecular Geometry Program. *J. Appl.Crystallogr.*, 2003, **36**, 7−13.

17 L. J. Farrugia, *J. Appl. Crystallogr.*, 1997, **30**, 565.

18 L. J. Farrugia, *J. Appl. Crystallogr.*, 1999, **32**, 837.

19 (a) A. Biswas, M. G. B. Drew, J. Ribas, C. Diaz and A. Ghosh, *Eur. J. Inorg. Chem.*, 2011, 2405–2408; (b) J. Carranza, C. Brennan, J. Sletten, F. Lloret and M. Julve, *J. Chem. Soc., Dalton Trans.*, 2002, 3164–3170.

20 S. Biswas and A. Ghosh, *Polyhedron*, 2012, **39**, 31–37.

21 (*a*) J. Ferguson, *J. Chem. Phys.*, 1961, **34**, 611−615; (b) M. P. Sigalas and C. A. Tsipis, *Inorg. Chem.*, 1986, **25**, 1875−1880.

22 E. M. Boge, D. P. Freyberg, E. Kokot, G. M. Mockler, E. Sinn, *Inorg. Chem.*, 1977, **16**, 1655−1660.

23 (a) M. Dey, C. P. Rao, P. K. Saarenketo and K. Rissanen, *Inorg. Chem. Commun.*, 2002, **5**, 924−928; (*b*) S. Banerjee, M. G. B. Drew, C.-Z. Lu, J. Tercero, C. Diaz and A. Ghosh, *Eur. J. Inorg. Chem.*, 2005, 2376−2383.

24 A. W. Addison, T. N. Rao, J. Reedjik, J. van Rijn and C. G. Verschoor, *J. Chem. Soc., Dalton Trans.*,1984, 1349−1356.

25 L. Yang, D. R. Powell and R. P. Houser, *Dalton Trans.*, 2007, 955−964.

26 J. J. Borrás-Almenar, E. Coronado, J. Curely and R. Georges, *Inorg. Chem.*, 1995, **34**, 2699–2704.

27 (*a*) M. A. Halcrow, J.-S. Sun, J. C. Huffman and G. Christou, Inorg. Chem., 1995, **34**, 4167–4177; (*b*) J. M. Clemente-Juan, B. Chansou, B. Donnadieu and J. P. Tuchagues, *Inorg. Chem.*, 2000, **39**, 5515–5519.

28 S. Shit, M. Nandy, G. Rosair, C. J. Gómez-García, J. J. Borras Almenar and S. Mitra, *Polyhedron*, 2013, **61**, 73−79.

29 C. Paraschiv, J.-P. Sutter, M. Schmidtmann, A. Müller, M. Andruh, *Polyhedron*, 2003, **22**, 1611−1615.